Indian Journal of Chemical Technology
Vol. 31, March 2024, pp. 222-232
DOI: 10.56042/ijct.v31i2.3962

Adsorptive removal of 2, 4 dichlorophenol by polysulfone/graphene oxide blended microcapsules immobilized with CYPHOS® IL 103 ionic liquid

S. Pandiarajan[1]*, S. Venkatesan[2] & K. Balasubramani[3]

[1]Department of Chemical engineering, Nandha Engineering College, Erode, Tamil Nadu, India

[2]Department of Petrochemical technology, University College of Engineering, Bharathidasan Institute of Technology campus, Anna university, Tiruchirappalli, Tamil Nadu, India

[3]Department of Chemical Engineering, Hindusthan College of Engineering and Technology, Coimbatore, Tamil Nadu, India

*E-mail id:pandiarajan87@gmail.com

Received 30 July 2023; accepted 30 January 2024

2,4-Dichlorophenoxyacetic acid (2,4-D), a phenoxyalkanoic acid herbicide, is among the most widely distributed pollutants in the environment. 2,4-Dichlorophenol (2,4-DCP), as the main metabolite which frequently detected in the environment resources. The toxicity of 2,4-DCP is more severe than that of its parent 2,4-D at any concentration levels. In this study, removal of 2,4-DCP from aqueous solution using graphene oxide (GO) + Trihexyl(tetradecyl) phosphoniumdecanoate [CYPHOS® IL 103] ionic liquid entrapped in polysulfone (PSF) capsule as an adsorbent (GO/IL/PSF microcapsule) is reported. Various techniques such as X-Ray diffraction, Fourier transform infrared spectroscopy, Field emission scanning electron microscopy and Brunauer-Emmett-Teller have been used to identify and confirm the formation of GO, functional group, surface morphology and surface area of the capsule. The adsorption capacity has been investigated under different experimental conditions including pH (2-10), initial 2,4-DCP concentration (20-100 mg L^{-1}), temperature (293-313 K) and at 250 rpm. It has been found that 97% of 2,4-DCP removed from aqueous solutions with adsorption capacity (q_e) of 388 $mg.g^{-1}$ at optimized experimental conditions. The equilibrium adsorption of 2,4-DCP on capsule can be best described by Langmuir isotherm model, with a maximum adsorption capacity (q_{max}) of 398 $mg.g^{-1}$ at room temperature. The adsorption kinetics is well described by the pseudo-second-order kinetic model than pseudo first order model and Freundlich kinetic. These results shows that capsule have promising application for adsorption of 2,4-DCP from aqueous solution.According to desorption research, the IL/GO/PSF may be renewed six times with a 1 N sodium hydroxide solution. IL/GO/PSF microcapsule is appropriate for use in fixed bed columns, which treat huge volume of wastewater.

Keywords: Adsorption, Graphene oxide, Ionic liquid, Isotherms, Phenolic compound, Polysulfone/graphene oxide blended microcapsules

Introduction

Environmental damage by phenolic elements in aquatic ecosystems encompasses a wide array of sources, including industrial effluents from various sectors, including gasoline, petroleum products, fuel transformation, varnishes, synthetic polymer epoxy, and the paper industry[1-3]. Such additives harm the health by adversely impacting the nervous system, digestive tract, eyelids, cardiovascular system, respiratory system, and spleen, as well as causing toxic effect, histological changes, genotoxicity, and carcinogenic effects[4].

Effluent containing phenolic compounds should be nullified before it can be used or disposed into accepting waterways[5,6]. In addition to the inherent substances, use of the pesticide 2,4-dichlorophenoxyacetic acid (2,4-D) across many agro-based crop production results in the formation of the 2,4-dichlorophenol (2,4-DCP) during degradation[7]. The consumption of 2,4-D as herbicide increases after chlorpyrifos[8]. Numerous tools have been used to remove phenolic compounds from aqueous phase, along with decomposition adsorbents, separation and purification, enzyme degradation, photo catalytic degradation[9].

Adsorption is a technique for removing contaminates from aqueous phase. Charcoal, recycled fibres and polyurethanes have mostly been studied as adsorbent materials[10]. The features of these adsorbents are their convenience of separation, uptake capacity, and modified for variety of materials separation[11]. Even though, there are obstacles, including intra-particle diffusion resistance and inadequate adhesion, adsorption serves as major

technique for separation of pollutants from fluids. Polymeric membrane, encapsulating with adsorbent have been employed in multiple areas[12].

Graphene oxide (GO) is also being used as common adsorbent, due to large surface area, outstanding chemical reliability, and good thermal stability[13,14]. Graphene oxide polymeric hybrid catalyst created attention of many researchers[15] due to excellent performance and wide range of applications. Polysulfone polymer (PSF) is widely used for production of substrates due to high thermal & chemical stability, high porosity and bio-compatibility[16,17].

Ionic liquids (ILs) are also viewed as an alternative green solvent. Specifically, room-temperature ILs are molten organic salts that are in a liquid state at or near room temperatures. They have received tremendous attention due to their excellent properties such as strong polarity, negligible vapour pressure, low volatility, thermal and chemical stability, designable structure, and a good ability to dissolve many inorganic, organic, and polymeric materials. Consequently, they have been used in the preparation of various membranes. Phosphonium-based Ionic liquid, such as trihexyl (tetradecyl) phosphonium (with chloride, bromide, decanoate, and bis (2,4,4-trimethylpentylphosphinate) anions) [CYPHOS® IL 103], have already been disclosed as beneficial organic solvent for separation of metallic ions and phenolic substances in aqueous phase[18]. IL cation has poor water solubility, which is significant property for preparation of graphene oxide +CYPHOS® IL 103 in polysulfone adsorbent. For separations processes, the absorbent should be easily separated from of the aqueous phase, as well as, appropriate for use in fixed bed columns, which treat huge volume of wastewater.

To the best of our knowledge, there are no reports related to phosphonium based IL CYPHOS IL103 and graphene oxide immobilized in polysulfone capsules for the removal of 2,4-dichlorophenol from aqueous solution. In this study, graphene oxide serves as adsorbent, polysulfone used as a polymer support matrix for preparing capsules. The CYPHOS IL103 is a carrier for the removal of 2,4-dichlorophenol.

Experimental Section

Materials

The analytical grade of 2,4-dichlorophenol (99% purity, Molecular weight – 163 g·mol^{-1}, Molecular formula - $Cl_2C_6H_3OH$, pKa -7.9) was obtained from Sigma Aldrich, India. The desirable concentrations of 2,4-DCP solutions were diluted from the stock solution obtained by the dissolution 1 g in 1000 mL of deionized water. The pH was altered by using NaOH and HCl using pH meter (Model Systronics-335). The concentration of 2,4-DCP in the aqueous solution was measured by 4-aminoantipyrine procedure (4-AAP) method using UV-visible spectrophotometer at a wavelength of 510 nm. Poly-sulfone (PSF) was obtained from Sigma Aldrich, India. The phosphonium-based ionic liquid trihexyltetradecylphosphonium decanoate ($C_9H_{19}COO$, ≥95% purity, solubility at (20 ± 1 °C) is 8.7 ± 0.2 mg/L) was purchased from sigma Aldrich, India. The structure is shown in Fig. 1. Dimethyl formamide (DMFA), sodium nitrate, potassium permanganate and the chemical reagents used for the experiments were of analytical grade.

Synthesis of graphene oxide

Modified Hummers method[19] was utilized for GO synthesis as follows: Graphite flakes (2 g), $NaNO_3$ (0.3 g) and $KMnO_4$ (4 g) was mixed thoroughly. The entire solution was mixed using sonication for 24 h and solution is turned as brownish paste. 100 mL of distilled water added to the paste to turn as yellow liquid with graphite solid. Hydrogen peroxide (1%) was added to arrest the reaction. The resultant yellow foam (GO) was purified by rinsing with distilled water, centrifuged with 5% hydrochloric acid, and further vacuum dried for usage.

Preparation of CYPHOS® IL 103/GO/PSF capsule

GO/PSF capsules were prepared from a solution containing polysulfone polymer and dimethylformamide (DMFA) solvent, using the phase

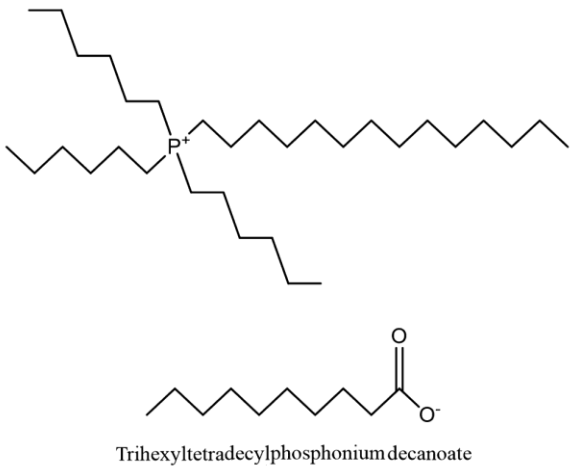

Fig. 1 — Structure of CYPHOS® IL 103 ionic liquid

inversion method[20]. The dispersed phase was prepared by dissolving 1.2 g of PSF, 0.1 g GO in 15.0 mL of DMFA, which was kept in an ultrasonic bath for 2 h for total dilution. After that the dispersed phase consisting of GO/PSF was injected with a 0.7 mm needle syringe at 3-4 cm above the continuous phase of 30% (v/v) ethyl alcohol aqueous solution[21]. In the aqueous solution, the droplets of GO/PSF precipitate were instantly formed as a capsule. A magnetic stirrer at 180 rpm was used to prevent agglomeration of the newly formed capsules. The capsules were rinsed with distilled water to remove dimethyl formamide and ethanol. After that, the capsules were ready for immobilisation of IL. 265.3 mg of GO/PSF capsules, 529.8 mg of IL, and 10.0 mL of methanol were added into an Erlenmeyer flask, which was kept under ultrasonic agitation for 2 h[21,22]. Then, the flask was placed on a heating plate nearly up to the total evaporation of the liquid, and the capsules were transferred to a sieve and rinsed with 2 L of distilled water to remove excess ionic liquid and dried[23].

Characterisation

The capsules were characterised using scanning electron microscopy (SEM, JSM-6390LV, Jeol, Japan). The surface area was calculated using the BET method (Autosorb-1, Quanta chrome Instruments, United States), samples were outgassed at 100 ℃ for 24 h to evacuate the physically adsorbed moisture before measurement. Fourier Transform Infrared Spectrometer (FT-IR, Cary 660, Agilent Technologies, United States) was used to acquire data between the wavenumbers 650 and 4000 cm^{-1}. The synthesized GO was analysed using X-Ray diffractometer (Bruker Axes D8 advance, USA) and the morphology of GO was investigated by transmission electron microscopy (TEM) (TECNAI F30 G2 S-TWIN).

Adsorption experiments

2,4-DCP with an initial concentration of 40 mg L^{-1} was prepared and then 10 mg of capsules were mixed into 100 mL of the sample and kept at 250 rpm for 3 h in a shaker. The 2,4-DCP of the adsorption capacity was measured by using q_e ($mg.g^{-1}$)

$$q_e = (C_0 - C_e) \times \frac{V}{m} \quad \text{... (1)}$$

$$\% \text{ removal of 2,4- DCP} = = \frac{C_0 - C_e}{C_0} \times 100 \quad \text{... (2)}$$

Where, qe is the quantity of 2,4-DCP adsorption per g of capsules (mg g^{-1}); C_o and C_e are the initial and final concentrations of the 2,4-DCP ($mg.L^{-1}$); V is the volume of solution (mL); m is the amount of capsule (g). In triplicate experiments, the influence of solution pH and temperature were investigated. For this, 10 mg of the prepared capsules were added to 100 mL of a 2,4-DCP solution and kept for 3 h at 250 rpm in a mechanical shaker (CE-720, Cienlab, Brazil). Triplicate experimental tests data were used to study adsorption kinetics and isotherm analysis.

Adsorption isotherms, kinetics and thermodynamics

Adsorption interactions isotherms, kinetics and thermodynamics are determining the 2,4-DCP binding nature in the prepared Capsule. The batch adsorption data were fitted to the isotherm (Henry, Langmuir, Freundlich, Dubinin-Radushkevich, Redlich-Peterson, Sips, Fritz–Schluender-III, Fritz–Schlunder-IV, Fritz–Schlunder-V) and kinetic (pseudo first order, pseudo second order, modified Freundlich) model using a nonlinear curve fitting method which was based on the "sum of normalized errors" (SNE) principle[24]. The numerical parameter such as Sum of absolute errors (EABS) were in use of objective function nonlinear regression analysis of model fitting, hybrid fractional error function (HYBRID), root-mean-square error (RMSE) were estimated to assess the goodness of the fits, Marquardt's percentage standard deviation (MPSD), sum of the square error (ERRSQ), nonlinear chi-square test (χ^2) and Coefficient of determination (R^2). To assess the viability and exothermic nature of the adsorption process, thermodynamic characteristics are required. Using van't Hoff's equation, the values of the thermodynamic parameters ΔS^0 and ΔH^0 were computed as follows: :

$$\ln K_c = \frac{\Delta S^0}{R} - \frac{\Delta H^0}{RT}$$

Where, Kc is Langmuir's constant (L mol^{-1}), R is the gas constant, 8.314 (J mol^{-1} K^{-1}), T is the temperature (K), ΔS^0 denotes the standard entropy change (J mol^{-1} K^{-1}), and ΔH^0 is the standard enthalpy (J mol^{-1}). The Gibbs free energy change (ΔG^0) was calculated from the Gibbs-Helmholtz equation, using values of van't Hoff's equation.

Results and Discussion

Characterization of graphene oxide +CYPHOS® IL 103 entrapped in polysulfone adsorbent

X-Ray diffraction analysis

The yield of GO from modified Hummers method was investigated by using XRD pattern which is shown in Fig. 2. Commonly, XRD patterns of high

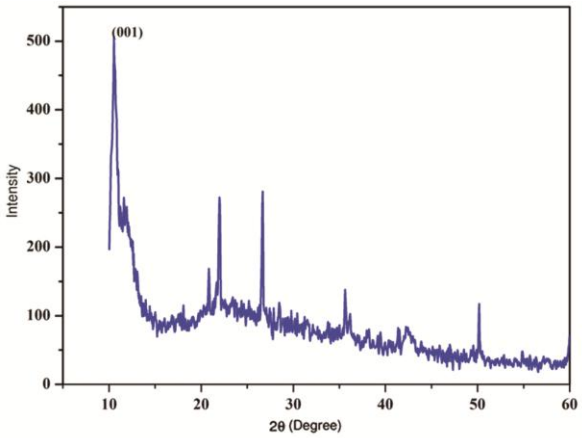

Fig. 2 — XRD pattern of synthesized graphene oxide

quality monolayer graphene should not contain any diffraction peaks due to its 2-D structure. However, weak diffraction peaks are typically observed for the synthesized graphene[25]. In this study, the XRD pattern of graphene shows low intensity peak in the plane (001) appear at 2θ =10.11° indicating that the entire graphite was exploited into sheets and thoroughly oxidised. The low intensity peaks between 20-30° could be small amount of impurities due to the presence of graphite[26].

FTIR spectral analysis

The FT-IR spectra in Fig. 3 give the specific molecular vibrations in the prepared capsules. The spectrum of pure PSF capsules (Fig. 3a) shows bands at 1632 cm^{-1}, 1412 cm^{-1} are because of asymmetric O=S=O stretching of sulfone group, the stretching vibrations of aromatic C=C groups are seen at 1317 cm^{-1} and 1043 cm^{-1}. Bands at 882 cm^{-1}, 807 cm^{-1} are due to aromatic ring vibrations. Fig. 3b implies the GO incorporated PSF capsules due to strong oxidation of graphene oxide the carboxyl C=O stretching vibration band at 1639 cm^{-1} and bands of 1296 cm^{-1}, 1043 cm^{-1} were observed for hydroxyl O-H deformation and carbonyl functional groups C=O stretching vibration[27]. The combination of graphene oxide with polysulfone observed at the bands at 882 cm^{-1}, 807 cm^{-1} stretching vibration. The spectrum shown in Fig. 3c for the IL/GO/PSF before adsorption has IL characteristics bands at 1362 cm^{-1} (stretching vibration P^{+}-O^{-}) and 898 cm^{-1}, 803 cm^{-1} (stretching vibration P–C). After adsorption of 2,4-DCP in the capsule there is no significant changes were identified in the FTIR spectrum shown in Fig. 3d. Slight variation in the band vibration of 1368 cm^{-1} (stretching vibration) and 899 cm^{-1} (stretching vibration P–C) due to the 2,4-DCP adsorption on adsorbent capsule[28,29].

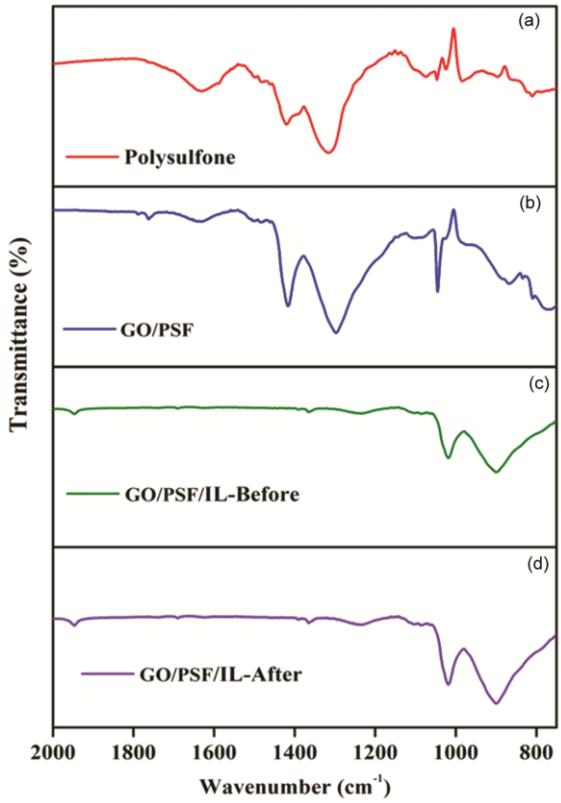

Fig. 3 — FTIR spectra of (a) poly-sulfone capsules, (b) PSF/GO capsules, (c) PSF/GO capsules coated with ionic liquid (before adsorption) and (d) PSF/GO capsules coated with ionic liquid (after adsorption)

Morphological observation

SEM is an effective way to analyse the internal and external morphological structure of PSF capsules[6]. Fig. 4a shows that a spherical rougher surface is and the cross section view shows its porous structure. A great interaction between the sorbents and the 2,4-DCP in water is created by the PSF capsules' large surface area. Figs 4b and 4c are the SEM images of the PSF/GO capsules without and with ionic liquid, respectively. In Fig. 4b, since GO blocks a part of pores, the surface area of capsules encapsulated with it is quite lower than that of capsules without it. On the surface of the PSF@GO capsules, there are still a lot of pores that are evenly distributed, which is seen from further SEM images and also the number of holes increased while their size has lowered. GO was almost uniformly distributed from the exterior surface to the interior of the GO/PSF capsule by seeing the tiny GO particles within the capsules[30]. Following ionic liquid immobilization Fig. 4c shows capsules

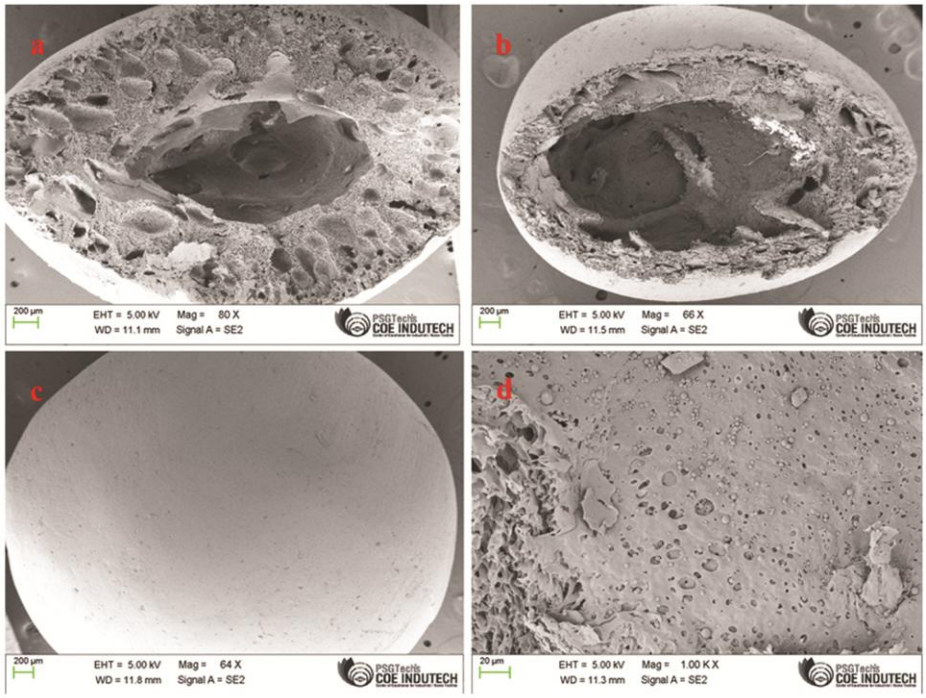

Fig. 4 — SEM images of (a) pure polysulfone capsules, (b) GO/PSF capsules, (c) GO/PSF capsules coated with ionic liquid (before adsorption) and (d) GO/PSF capsules coated with ionic liquid (after adsorption)

with high porosity, a consistent structure, and a smoother outer layer, which improves the availability of the formed porous structure. The developed pores are clearer to after the capsule immobilized with ionic liquid. Fig. 4d shows capsules following 2,4-DCP adsorption; 2,4-DCP molecules can be found in the larger pores and on the exterior of the capsules[17,31].

TEM analysis

The TEM images of CYPHOS® IL 103/GO/PSF capsule shown in Fig. 5 demonstrated that the PSF/GO surface was evenly covered in CYPHOS® IL 103. The uniform dispersion of IL on PSF/GO surface, with minimal aggregation, verified that PSF/GO had been decorated with IL, and PSF/GO offered strong support for IL blooming and distribution[24].

BET surface area analysis

BET surface analysis (Fig. 6) of prepared capsules indicates mesoporous in nature and possessed large surface of area of 117.4 m^2 and 176.6 m^2g^{-1} with inter-particle pore size 10.50 nm and 0.278 cm^3/g pore volume accordingly[32].

Adsorption experiments

Effect of pH

As the solution pH mainly influences the adsorption 2,4-DCP by capsules, experiments were conducted at pH 2 to 10 and the results are presented in Fig. 7a. The maximum adsorption capacity was found to be 388 $mg.g^{-1}$ at pH 6, after that the medium was unfavourable for the adsorption process. The ionic fraction of the chlorophenolate ion increased with increasing pH, and 2,4-DCP became negatively charged as the pH increased, as well as the

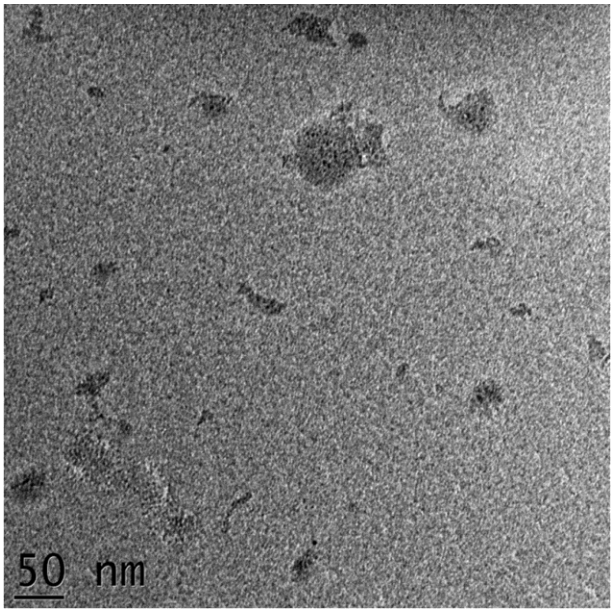

Fig. 5 — TEM image of CYPHOS® IL 103/GO/PSF capsule

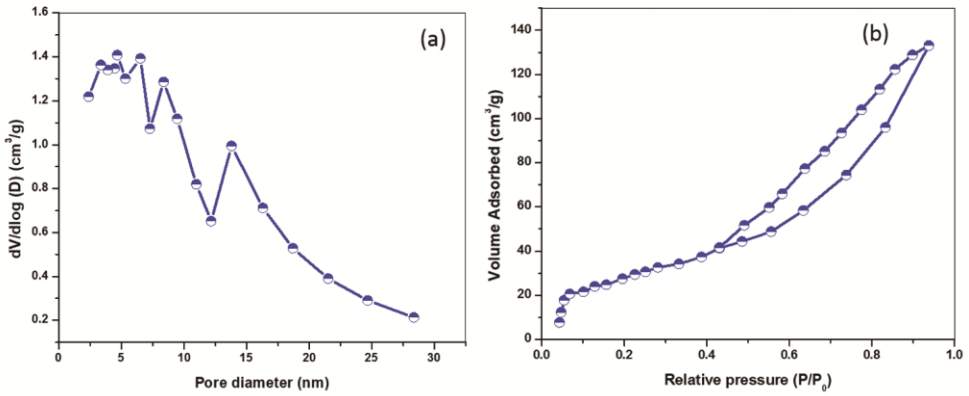

Fig. 6 — (a) BET isotherm and (b) pore volume vs pore diameter plot of graphene oxide incorporated polysulfone capsules

phosphonium in the ionic liquid, repelled one another electrostatically when pH >pKa (pKa = 7.89 for 2,4-DCP). Furthermore, the dissociation of 2,4-DCP results in a reduction in hydrophobicity since the attraction of chlorophenols for the capsule surface is also diminished[33]

Effect of temperature

At three different temperatures (293 K, 303 K, and 313), various initial concentrations of 2,4-DCP that varied from 20 to 60 mg/L were prepared and investigated. The adsorption of 2,4-DCP decreased as the temperature increased as shown in Fig. 7b, indicating that the adsorption reactions are exothermic. Regarding temperature, increasing the system temperature may lead to an eventual decrease in analyte-capsule interactions, which in turn could lead to a decrease in adsorption[14].

Effect of initial concentration

For the purpose of assessing the effect of initial concentration, the most optimal conditions of pH 6, 303 K, and 250 rpm were maintained. The result of the experiment showed that the removal % of 2,4-DCP decreases with increasing temperature and initial concentration as shown in Fig. 8. The best removal was achieved at 303 K with a 20 mg/L initial concentration. The surface area and the number of available adsorption sites were comparatively high when the initial concentration was low. As a result, adsorbent capsules may retain more 2,4-DCP. As the analyte concentration gets higher, the area surrounding the capsule's active site becomes saturated, which can result in either a constant or decreasing removal percentage of 2,4-DCP[34].

Regeneration of capsule

The GO/PSF capsule coated with ionic liquid must have a good recycling rate and an acceptable

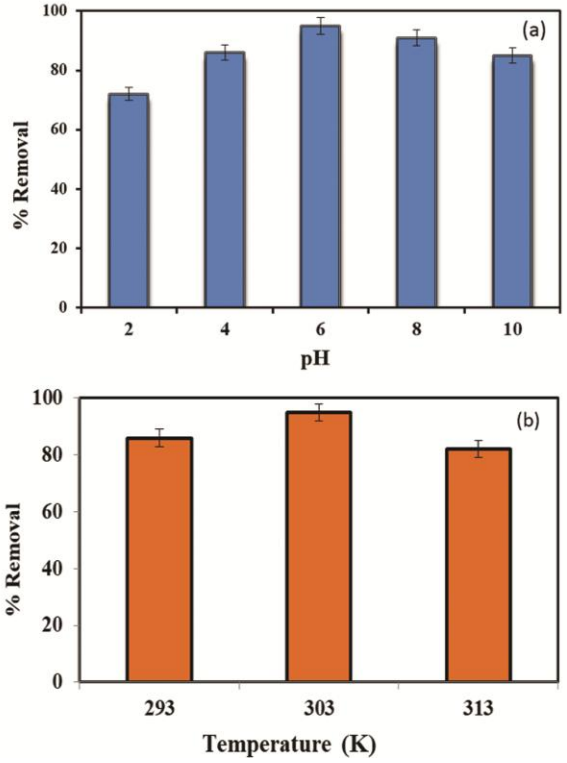

Fig. 7 — Effect of (a) solution pH and (b) temperature on % removal (pH 6.0, Temperature = 303K, 250 rpm)

adsorption capacity for use in real applications. 2,4-DCP adsorbed onto IL/GO/PSF capsule was treated with 1 N NaOH to desorb 2,4-DCP and repeated for 6 desorption cycles in Fig. 9. It demonstrated that NaOH has higher regeneration efficiency than other solvents since it is replaced the 2,4-DCP ions on the IL/GO/PSF capsule surface alongside OH^- ions. It additionally derived that the desorption capacity of NaOH decreased slightly (±8%) during each regeneration cycle because of the

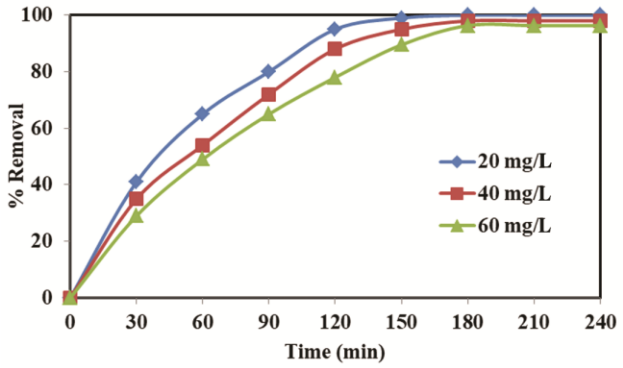

Fig. 8 — Effect of initial concentration on % removal (pH 6.0, Temperature = 303 K, 250 rpm)

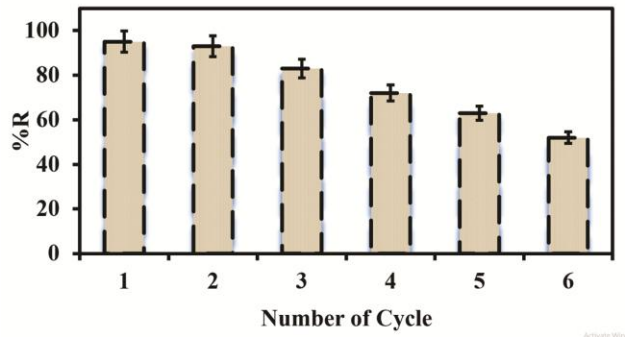

Fig. 9 — Regeneration of IL/GO/PSF using NaOH

loss of IL/GO/PSF particles during washing and the progressive elimination of surface functional groups. It was reasonable to assume that the regenerated IL/GO/PSF was possibly used a maximum of five times for 2,4-DCP adsorption[35].

Adsorption analysis of isotherms, kinetics and thermodynamics

Isotherms

The experimental investigation data on 2,4-DCP adsorption over prepared capsule was fitted to several parameter isotherms. The adsorption parameters were determined by minimising the selected error function, which resulting in small SNE values. The isotherms optimal parameters and related statistical parameters were provided in Table 1. One parameter for Henry's model was not correlating the data, as this model is only applicable for dilute solutions, as shown in Table.1. Among the two-parameter isotherm model Langmuir[36], Freundlich[37] and Temkin[38] were correlated to optimal parameter of their small SNE values. The Freundlich isotherm, is one of the two parameter models, provided a reasonable fit to the experimental data, revealing that 2,4-DCP was adsorbed in multilayers onto IL/GO/PSF capsule after chemisorption (1/nF =0.27). Langmuir which gives the maximum adsorption capacity of 2,4-DCP onto prepared capsule is 388 mg/g and error function is ERRSQ gives the small SNE values of 4.89. Three parameters isotherm model fit the data more effectively than the other four models for the both Sips and Fritz–Schluender-III equations. Sips isotherm is well fit; 2,4-DCP concentration was high in bulk solutions during the early period of time, followed by multilayer adsorption. The fitness order of the three parameter isotherms is as follows, based on correlation coefficients and chi square values: Fritz–Schluender-III > Sips > Khan > Redlich-Peterson >. The adsorption data, which is known by the R^2 (0.9881) values, was obeyed by four selected models of four parameters. When the RMSE and χ^2 values were compared, it was revealed that the Weber-van Vliet isotherm fit the adsorption data well, with small RMSE (11.62) and χ^2 (2.65), showing that 2,4-DCP was adsorbed in multilayers onto prepared capsule by van der Waals binding. The 2,4-DCP adsorption data were quite well fit using the Fritz–Schluender-V five parameter isotherm [26], which has significant coefficient of determination (R^2 0.9989), root-mean-square error (RMSE 0.26) and nonlinear chi-square test (χ^2 0.001).

Kinetics

The kinetics of 2,4-DCP adsorption onto prepared capsule was investigated using well-known pseudo first order, pseudo second order and Modified Freundlich kinetic models at various initial concentrations[39]. The SNE values and kinetic data for different initial concentration circumstances (20 – 100 mg/L) are shown in Table 2. With high R^2 (0.9990–0.9887), RMSE (4.261–32.682), and χ^2 (0.329–986), the pseudo II order model fit the kinetic data better than the pseudo I order model and Freundlich kinetic. Clearly, the % removal reached over 80% in 120 min, followed by a slower adsorption until the adsorption equilibrium was reached at around 180 min. It confirmed the isotherm analysis findings by indicating the chemisorptive nature of 2,4 - DCP on prepared capsule for adsorption. At low initial concentrations, the equilibrium concentration (C_e) values were low, but as the final concentrations increased, the (C_e) values raised. This phenomenon might be attributed to cooperative diffusion at high starting concentrations, as confirmed by the isotherm analysis[40].

Thermodynamics

The thermodynamic characteristics of 2,4-DCP adsorption nature onto the capsules was deduced from

Table 1 — 2,4-DCP onto prepared capsule using Optimal isotherm, statistical parameters, error function & small SNE values for different isotherms

Isotherm	Constants	Values	R^2	RMSE	χ^2	ERROR	SNE
Henry $q_e = k_H C_e$	H (L/mg)	2.60	0.5688	101.95	21.54	ERRSQ	4.03
Langmuir	b_L(L/mg)	0.59					
$q_e = \frac{q_m b C_e}{1 + b C_e}$	q_m(mg/g)	398	0.9673	112.70	49.02	ERRSQ	4.89
	K_L	0.01					
Freundlich	K_f (L/g)	53.29					
$q_e = K_f C^{1/n}$	n_F	3.62	0.9778	76.60	32.42	MPSD	4.35
Dubinin-Radushkevich	q_{mDR} (mg/g)	109.27					
$q_e = q_{mDR} exp[-K_{DR}(RTln\left(1+\frac{1}{C_e}\right)^2)]$	K_{DR}	0.001	0.9062	128.53	54.32	EABS	4.89
	E	21.45					
Redlich-Peterson	K_{RP1}(L/g)	52.40					
$q_e = \frac{K_{RP\,1} C_e}{1 + K_{RP\,2} C_e^{\beta_{RP}}}$	K_{RP2} (L/mg)	98.49					
	β_{RP}	0.52	0.9551	62.25	23.85	HYBRD	4.79
Sips	b	0.21					
$q_e = \frac{b q_{ms} C_e^{1/n}}{1 + b C_e^{1/n}}$	q_{ms}(mg/g)	186.08					
	n	3.33	0.9801	52.43	61.51	EABS	4.65
Fritz–Schluender-III	K_{FS3q_m} (mg/g)	146.05					
$q_e = \frac{K_{mFS} K_{FS} C_e}{1 + K_{mFS} C_e^{n_{FS}}}$	K_{FS}	2.13					
	n_{FS}	0.71	0.9913	61.04	9.42	ARE	4.12
Fritz–Schlunder-IV	K_{FS4q_m}(mg/g)	15.27					
$q_e = \frac{K_{FS} q_m C_e}{1 + qsm C_e^{\alpha}}$	qsm	4.57					
	a	0.04					
	b	4.65	0.9653	16.08	16.02	MPSD	4.87
Weber–van Vliet	P_1	4.79					
$C_e = P_1 q_e^{(P_{2q_e^{p3}+p_4})}$	P_2	0.02					
	P_3	0.65					
	P_4	2.77	0.9881	11.62	2.65	ERRSQ	4.01
Fritz–Schlunder-V	K_{FS5q_m} (mg/g)	86.26					
$q_e = \frac{q_{mFSS} K_1 C_e^{m1}}{1 + K_2 C_e^{m2}}$	K_1	1.09					
	m_1	0.44					
	K_2	0.78					
	m_2	0.41	0.9989	0.26	0.001	MPSD	4.21

Table 2 — 2,4-DCP onto prepared capsule using small SNE values obtained and the respective error functions for different kinetics

Model	Parameter	20 (mg/L)	40 (mg/L)	60 (mg/L)	80 (mg/L)	100 (mg/L)
Pseudo first order	K_1^t (1/min)	0.009	0.015	0.019	0.055	0.065
$q = q_e(1 - \exp^{-K_1 t}I$	C_e (mg/L)	0.4	1.8	3.4	5.0	7.0
	R^2	0.9881	0.9978	0.9819	0.9861	0.9982
	RMSE	5.023	17.084	26.280	36.195	46.082
	χ^2	0.822	1.420	1.802	3.035	6.067
	ERROR	MPSD	ERRSQ	EABS	HYBRD	EABS
	SNE	4.06	4.82	4.51	4.06	4.90
Pseudo second order	C_e (mg/L)	0.3	1.3	2.8	4.3	0.64
$q = \frac{q_e^2 kt}{1 + kq_e t}$	$K_{I,Ho}$(g/mg min)	2.03×10^{-05}	4.08×10^{-06}	5.09×10^{-06}	5.88×10^{-06}	3.35×10^{-06}
	R^2	0.9887	0.9893	0.9895	0.9854	0.9990
	RMSE	4.261	12.194	18.059	24.656	32.682
	χ^2	0.329	0.567	0.674	0.393	0.986
	ERROR	ARE	EABS	ERRSQ	HYBRD	MPSD
	SNE	4.15	4.22	4.51	4.67	4.50
Modified Freundlich	m_f	4.5840	3.0941	2.7312	1.4828	0.9759
$q_t = k_{mf} t^{1/m_f}$	K_{mf}	0.1842	0.1762	0.1989	0.0995	0.0984
	R^2	0.9888	0.9786	0.9980	0.9831	0.9989
	RMSE	6.05	9.06	11.29	18.51	24.87
	χ^2	0.1005	0.1894	0.2967	0.4060	0.5111
	ERROR	MPSD	EABS	ERRSQ	HYBRD	ARE
	SNE	4.05	4.62	4.21	4.07	4.01

Table 3 — 2,4-DCP adsorption onto prepared capsule for thermodynamic parameters in different temperature

T (K)	IL/GO/PSF capsule		
	ΔG° (KJ mol^{-1})	ΔH° (KJ mol^{-1})	ΔS° (KJ mol^{-1} K^{-1})
293	-155.57		
303	-161.65	-2.12	4.66
313	-189.26		

the results of adsorption experiments performed at 293, 303, and 313 K. 2,4-DCP. The thermodynamic parameters including changes in the standard enthalpy (ΔH°), the Gibbs free energy (ΔG°), and the standard entropy (ΔS°) were calculated at different temperatures (293–313 K) are seen in Table 3. At all temperatures, the results of (ΔG°) were negative, indicated spontaneity of the adsorption process[41]. According to the negative (ΔH°) value, the adsorption reaction was exothermic, 2,4-DCP adsorption was more efficient at room temperatures and reduced as temperature increased. Also, throughout the adsorption process, the positive (ΔS°) value suggested enhanced randomness at the adsorbate-capsule interface[29].

Conclusion

The investigation of batch adsorption of 2,4-DCP from an aqueous solution was carried out. Here, a polysulfone capsule encapsulated with graphene oxide which is immobilised with ionic liquid is utilised as an adsorbent. Graphene oxide was synthesized using a modified Hummers approach. The prepared capsule was characterized through the use of XRD, FTIR, FESEM, and BET surface area analyzer, the synthesized capsule was characterized. XRD confirms the graphene oxide formation, FTIR identified the function groups in capsule, FESEM confirmed the uniform distribution of GO and smooth coating of Ionic liquid in the capsule. Systematically investigated the effects of initial 2,4-DCP concentration, temperature, adsorption time, and solution pH on 2,4-DCP adsorption characteristics. The optimum adsorption conditions were pH 6.0, 180 min of adsorption period, and 30 °C. it was observed that 97% of 2,4-DCP removed from aqueous solutions with adsorption capacity (q_e) of 388 mg/g at optimized experimental conditions. The highest adsorption capacity (q_m) was 398 mg/g according to the adsorption isotherm data, which is based on the Langmuir isotherm model. The pseudo-second-order kinetic model is confirmed by the adsorption's kinetic data. The exothermic nature of the process was confirmed by the thermodynamic analysis of 2,4-DCP adsorption making use of capsule. Gibb's free energy values being negative demonstrate that the process was quite spontaneous. Change in entropy's positive value (ΔS^o = 4.66 kJ/mol K) implies that the solution/solid interface's randomness became greater. Reusability tests showed that IL/GO/PSF could be successfully regenerated six times with a diluted NaOH solution before being used again. This study evidenced a large potential use of IL/GO/PSF as an adsorbent for 2,4-DCP removal.

Acknowledgment

The authors are thanks to Department of Petrochemical technology, University College of Engineering, Bharathidasan Institute of Technology Campus, Anna University, Tiruchirappalli, for providing facilities and carried our research work

References

1 Akhtar M, Bhanger M I, Iqbal S & S M Hasany, Sorption potential of rice husk for the removal of 2 , 4-dichlorophenol from aqueous solutions : Kinetic and thermodynamic investigations, *J Hazard Mater*, 128 (2006) 44.

2 Antonio P, Iha K & Suárez-Iha M E V, Kinetic modeling of adsorption of di-2-pyridylketone salicyloylhydrazone on silica gel, *J Colloid Interf Sci*, 307 (2007) 24.

3 Archana V, Begum K M M S & Anantharaman N, Studies on removal of phenol using ionic liquid immobilized polymeric micro-capsules, *Arab J Chem*, 371 (2013) 9.

4 Bekiaris G, Peltre C, Jensen L S & Bruun S, Molecular and biomolecular spectroscopy using FTIR-photoacoustic spectroscopy for phosphorus speciation analysis of biochars, *Spectrochim Acta Part A*, 168 (2016) 29.

5 Lin S & Juang R, Adsorption of phenol and its derivatives from water using synthetic resins and low-cost natural adsorbents : A review, *J Environ Manage*, 90 (2009) 1336.

6 Bilgin E, Ivan S, Sausa O & D Berek, Microporous carbon fibers prepared from cellulose as efficient sorbents for removal of chlorinated phenols, *Res Chem Intermed*, 43 (2016) 503.

7 Vidyavathy M S, Effect of process parameters on the phenol removal rate from petrochemical effluents using electrochemical method, *J Chem Pharm Res*, 8 (2016) 529.

8 Muthusaravanan S, Balasubramani K, Suresh R, Ganesh R S, Sivarajasekar N, Arul H, Rambabu K, Bharath G, Sathishkumar V E, Murthy A P & Banat F, Adsorptive removal of noxious atrazine using graphene oxide nanosheets : Insights to process optimization, equilibrium, kinetics, and density functional theory calculations, *Environ Res*, 200 (2021) 111428.

9 Zhang R, Li Y, Wang Z, Tong Y & Sun P, Biochar-activated peroxydisulfate as an effective process to eliminate pharmaceutical and metabolite in hydrolyzed urine, *Water Res*, 177 (2020) 115809.

10 Balasubramani K, Sivarajasekar N, Muthusaravanan S, Ram K, Naushad M, Ahamad T & Sharma G, Efficient

removal of antidepressant Flupentixol using graphene oxide/cellulose nanogel composite: Particle swarm algorithm based artificial neural network modelling and optimization, *J Mol Liq*, 319 (2020) 114371.

11 Fan J, Fan Y, Pei Y, Wu K, Wang J & Fan M, Solvent extraction of selected endocrine-disrupting phenols using ionic liquids, *Sep Purif Technol*, 61 (2008) 324.

12 Wang Z, Li X, Wang L, Li Y, Qin J, Xie P, Qu Y, Sun & Fan R, Flexible multi-walled carbon nanotubes / polydimethylsiloxane membranous composites toward high-permittivity performance, *Adv Compos Hybrid Mater*, 3 (2020) 1.

13 Balasubramani K, Sivarajasekar N & M Naushad, Effective adsorption of antidiabetic pharmaceutical (metformin) from aqueous medium using graphene oxide nanoparticles: Equilibrium and statistical modelling, *J Mol Liq*, 301 (2020) 112426.

14 Liu Q, Shi J, Zeng L, Wang T, Cai Y & Jiang G, Evaluation of graphene as an advantageous adsorbent for solid-phase extraction with chlorophenols as model analytes, *J Chromatogr A*, 1218 (2011) 197.

15 Ferreira A, Mota A, Oliveira A, Rodrigues F, Pacifico S, Da Silva J, Abagaro , Saraiva G, De Castro A, Teixeira R & Sousa N V, Equilibrium and kinetic modelling of Adsorption : Evaluating the performance of an adsorbent in softening water for irrigation and animal consumption, *Rev Virtual Quim*, 11 (2020) 1752.

16 Gong X C, Luo G S, Yang W W & Wu F Y, Separation of organic acids by newly developed polysulfone microcapsules containing triotylamine, *Sep Purif Technol*, 48 (2006) 235.

17 Han D & Row K H, Recent applications of ionic liquids in separation technology, *Molecules*, 15 (2010) 2405.

18 Pandiarajan S & Venkatesan S, Removal of 2,4-dichlorophenol using ionic liquid [BMIM]+[PF6]-encapsulated PVDF membrane, *J Indian Chem Soc*, 100 (2023) 100781.

19 William S, Hummers J R & Offeman R E, Preparation of graphitic oxide, *J Am Chem Soc*, 80 (1958) 1339.

20 Berg C V D, Roelands C P M, Bussmann P, Goetheer E L V, Verdoes D & Van D W L A M, Reactive & Functional Polymers Preparation and analysis of high capacity polysulfone capsules, *React Funct Polym*, 69 (2009) 766.

21 Ma X, Li Y, Li X, Yang L & Wang X, Preparation of novel polysulfone capsules containing zirconium phosphate and their properties for Pb2+ removal from aqueous solution, *J Hazard Mater*, 188 (2011) 296.

22 Kazak O, Tor A, Akin I & Arslan G, Preparation of new polysulfone capsules containing Cyanex 272 and their properties for Co(II) removal from aqueous solution, *J Environ Chem Eng*, 3 (2015) 1654.

23 Abu-Nada A, Abdala A & McKay G, Removal of phenols and dyes from aqueous solutions using graphene and graphene composite adsorption: A review, *J Environ Chem Eng*, 9 (2021) 105858.

24 Balasubramani K, Sivarajasekar N, Sarojini G & Naushad M, Removal of antidiabetic pharmaceutical (Metformin) using graphene oxide microcrystalline cellulose (GOMCC): Insights to process optimization, equilibrium, kinetics, and machine learning, *Indian Eng Chem Res*, 62 (2023) 4713.

25 Garba Z, Zhou W, Lawan I, Xiao W, Zhang M, Wang L, Chen L & Yuan Z, An overview of chlorophenols as contaminants and their removal from wastewater by adsorption: A review, *J Environ Manage*, 241 (2019) 59.

26 Nethaji S, Sivasamy A & Mandal A B, Adsorption isotherms, kinetics and mechanism for the adsorption of cationic and anionic dyes onto carbonaceous particles prepared from Juglans regia shell biomass, *Int J Environ Sci Technol*, 10 (2013) 231.

27 Sobon G, Sotor J, Jagiello J, Kozinski R, Zdrojek M, Holdynski M, Paletko P, Boguslawski J, Lipinska L & Abramski K M, Graphene oxide vs reduced graphene oxide as saturable absorbers for Er-doped passively mode-locked fiber laser, *Opt Express*, 20 (2012) 19463.

28 Panizza M & Cerisola G, Direct and mediated anodic oxidation of organic pollutants, *Chem Rev*, 109 (2009) 6541.

29 Machado D B, Skoronski E, Soares C & Padoin N, Immobilisation of phosphonium-based ionic liquid in polysulfone capsules for the removal of phenolic compounds, with an emphasis on 2,4-dichlorophenol, in aqueous solution, *J Environ Manage*, 291 (2021) 112670.

30 Nasseri S, Ebrahimi S, Abtahi M & Saeedi R, Synthesis and characterization of polysulfone/graphene oxide nano-composite membranes for removal of bisphenol A from water, *J Environ Manage*, 205 (2018) 174.

31 Zhu G, Cheng G, Lu T, Cao Z, Wang L, Li Q & Fan J, An ionic liquid functionalized polymer for simultaneous removal of four phenolic pollutants in real environmental samples, *J Hazard Mater*, 373 (2019) 347.

32 Regti A, Laamari M R, Stiriba S E & El-Haddad M, Potential use of activated carbon derived from Persea species under alkaline conditions for removing cationic dye from wastewaters, *J Assoc Arab Univ Basic Appl Sci*, 24 (2017) 10.

33 Li Z, Wu M, Jiao Z, Bao B & Lu S, Extraction of phenol from wastewater by N -octanoylpyrrolidine, *J Hazard Mater*, 114 (2004) 111.

34 Ma J, Wang H, Wang F & Huang Z, Adsorption of 2,4-dichlorophenol from aqueous solution by a new low-cost adsorbent –activated bamboo charcoal, *Sep Sci Technol*, 45 (2015) 2329.

35 Ge X, Wu Z, Manzoli M, Wu Z & Cravotto G, Feasibility and the mechanism of desorption of phenolic compounds from activated carbons, *Indian Eng Chem Res*, 59 (2020) 12223.

36 Kowanga K D, Gatebe E, Mauti G O & Mauti E M, Kinetic, sorption isotherms , pseudo-first-order model and pseudo-second-order model studies of Cu (II) and Pb (II) using defatted Moringa oleifera seed powder, *Phytopharmocol J*, 5 (2016) 71.

37 Balasubramani K & Sivarajasekar N, Adsorption studies of organic pollutants onto activated carbon, *Int J Innov Res Sci Eng Technol*, 3 (2014) 10575.

38 Karthik V, Selvakumar P, Sivarajasekar N, Megavarshini P, Brinda N, Kiruthika J, Balasubramani K, Ahamad T & Nausad M, Comparative and Equilibrium Studies on Anionic and Cationic Dyes Removal by Nano-Alumina-Doped Catechol Formaldehyde Composite, *Chem J*, 2020 (2020) 15.

39 Coimbra R N, Escapa C & Otero M, Adsorption separation of analgesic pharmaceuticals from ultrapure and waste water: Batch studies using a polymeric resin and an activated carbon, *Polymers*, 10 (2018) 958.
40 Ozcan S, Tor A, Aydin M E, Beduk F & Akin I, Sorption of phenol from aqueous solution by novel magnetic polysulfone microcapsules containing Cyanex 923, *React Funct Polym*, 72 (2012) 451.
41 Rambabu K, Bharath G, Banat F & Show P L, Biosorption performance of date palm empty fruit bunch wastes for toxic hexavalent chromium removal, *Environ Res*, 187 (2020) 109694.